Mass Transfer and Chemical Reaction in Hollow-Fiber Membrane Reactors

K. Li
Dept. of Chemical Engineering, University of Bath, Bath BA2 7AY, U.K.

Xiaoyao Tan
Dept. of Chemical Engineering, Shandong Institute of Technology, Shandong Province, P. R. China 255012

Theoretical models developed describe hollow-fiber memebrane reactors (modules), in which membrane functions as an efficient reactant distributor and the chemical reaction takes place either in the hollow-fiber lumen or in the shell side. Effects of various design and operating parameters, and physical properties on the performance of the reactors were studied. Simulation results indicated that the axial dispersion has to be considered when the chemical reaction takes place in the shell side. It, however, may be neglected when Pe > 40. Theoretical results further revealed that the mass-transfer direction of the reactant through the membrane might be reversed when the chemical reaction in the liquid is extremely fast. Experimental data in the literature obtained from water-treatment processes agreed satisfactorily with the theoretical solutions. Based on the developed solution method, the reaction kinetic parameters can also be obtained conveniently.

Introduction

Selective permeation through a membrane has become a recognized chemical engineering process for separation of fluid mixtures. During the past two decades, considerable attention has been paid to the integration of the permeation process into chemical reactors. Membrane reactors, which combine reaction and separation or combine mixing/distribution and reaction in one-unit operation, are the result of this integration. These reactors have been used to enhance the reaction yield and conversion of thermodynamically limited reactions (Mohan and Govind, 1988) or to control the reaction pathway by introducing a reactant into the reaction zone in a controlled manner (Coronas et al., 1994a,b).

Use of memebrane reactors to shift the equilibrium in a reversible reaction has been recognized since the 1960s (Pfefferle, 1966; Wood, 1968; Michaels, 1968). The combined reaction and separation process first found its application in biological systems at low temperatures (Chang and Furusaki, 1991). In recent years, however, availability of ceramic or metallic membranes has extended its application to high-temperature catalytic reactions (Shu et al., 1991; Hsieh, 1991). A comprehensive analysis of equilibrium shift isothermal reactors with a permselective wall was given by Mohan and Govid (1988).

The use of membrane reactors to control the addition and distribution of a reactant has been mainly studied for partial oxidative reactions of hydrocarbons (Eng and Stoukides, 1992). The membrane, often a dense type, controls the oxygen reactant supply to the hydrocarbon compartment and avoids the direct presence of gas-phase oxygen, which is often deleterious to hydrocarbon selectivity, thus, in some degree, suppressing the deep oxidation of the hydrocarbons. Theoretical studies of a methane coupling reaction (Reyes et al., 1993a,b; Cheng and Shuai, 1995) predicted that a much better C_2 yields could be achieved in membrane reactors compared to conventional fixed-bed reactors. The use of membrane reactors also has advantages in controlling the hot spots in exothermic reactions (Tsai et al., 1995; Coronas et al., 1997).

In water-treatment processes, efficient and localized introduction of a reactant in a controlled manner using hollow-fiber membrane reactors, which have a high surface area per unit volume, can often lead to a much reduced mass-transfer

Correspondence concerning this article should be addressed to K. Li.

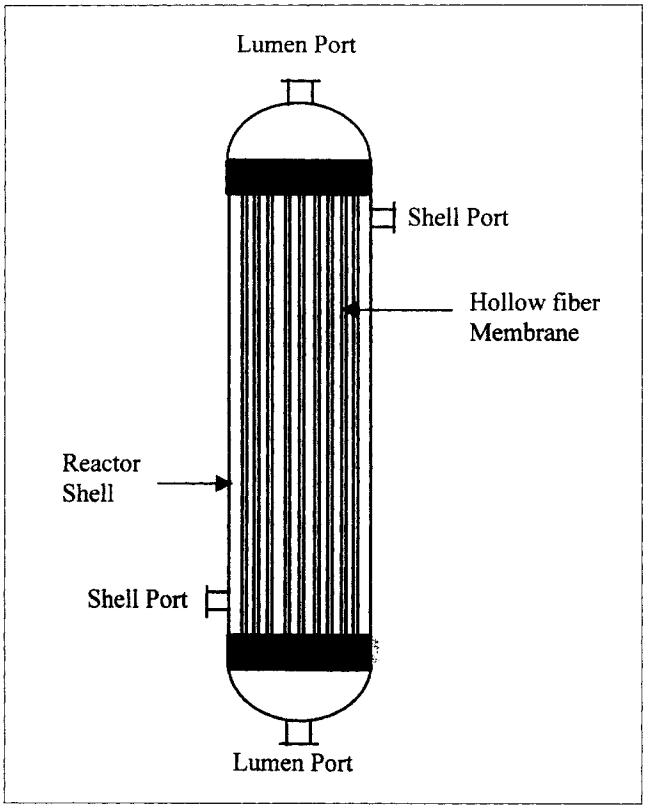

Figure 1. Hollow-fiber membrane module.

resistance, and hence can increase the overall efficiency of the water-treatment processes (Shanbhag et al., 1995, 1998). Li et al. (1995) investigated a novel membrane reactor for dissolved oxygen removal in ultrapure water production. Since, in their study, a microporous hollow-fiber membrane was used as an efficient gas distributor for bubbleless dissolution of hydrogen in the water, the reaction between the dissolved oxygen and hydrogen in water was enabled at excess hydrogen condition, and thus an extremely low DO level (less than 1.5 ppb) in water was achieved.

The purpose of this article is to provide a comprehensive analysis of a hollow-fiber membrane module (reactor) for contaminant removal from liquid. The membrane employed functioned not only as an efficient gas reactant distributor for gas/liquid reactions in liquid, but also as a stripper if the contaminants in liquid are gases. The model equations represent the hollow-fiber membrane reactors where a chemical reaction takes place either in the hollow-fiber lumen or in the shell side. The effects of various designing and operating parameters, and physical properties on the performance of the reactors, were studied in details.

Theory

Formulation of the model

The hollow-fiber membrane reactor is made up of n hollow fibers. As shown in Figure 1, the hollow fibers, assembled as a bundle, are encased in a tube and then are sealed at each end. The feed gas and liquid are introduced into the fiber lumen and the shell compartment, respectively, or vice versa. The gas reactant b is transferred through the membrane and then reacted with the reactant a in liquid in either the hollow-fiber lumen or in the shell side, depending on the operating modes. The following assumptions are adopted for the model development.

1. Constant density is considered for the liquid stream. This assumption approximates the liquid system realistically and simplifies the mass-balance equations considerably.
2. Fully developed laminar flow occurs if the liquid is in the fiber lumen. This assumption is usually valid for a Reynolds number not exceeding 2100. The entrance effect for the flow profile in the fiber lumen is ignored, because it is not significant compared to the length of the fiber used. Furthermore, the flow velocity in the fiber lumen can generally be expected to be greater than axial diffusion.
3. In the case where the liquid is introduced into the shell side, the dispersed plug-flow conditions is expected to prevail because of the packing of the hollow fibers in the module.
4. The reaction only occurs in liquid.
5. The system is operated isothermally and at steady state.

Based on these assumptions, the general mass-conservation equation for a reaction, which takes place either in the hollow-fiber lumen or in the shell side of the membrane reactor, can be established as follows.

Reaction in the Shell Side

$$u\frac{dC_i}{dz} - D_{Li}\frac{d^2C_i}{dz^2} + \frac{2}{R_o}\cdot k_{gi}\frac{1-\epsilon}{\epsilon}(C_i - p_i/H_i) + \upsilon_i k_r C_a C_b = 0 \qquad (i=a,b), \quad (1)$$

with the boundary conditions

$$z = 0, \qquad C_i = C_{i0} + \frac{D_{Li}}{u}\cdot\frac{dC_i}{dz} \qquad (1a)$$

$$z = Z, \qquad \frac{dC_i}{dz} = 0, \qquad (1b)$$

where u is the superficial velocity of the liquid stream (m/s); D_L is the axial dispersion coefficient (m^2/s); R_o is the outer radius of the hollow fiber (m); k_g is the mass-transfer coefficient (m/s); ϵ is the void fraction of the reactor defined by $\epsilon = 1 - n\pi d_o^2/4A$; n is the number of hollow fibers; d_o is the outer diameter of the hollow fiber (m); A is the cross-sectional area of the reactor (m^2); H_i is the Henry constant ($Pa\cdot m^3\cdot mol^{-1}$); p_i is the partial pressure in gas phase (Pa); k_r is the second-order reaction rate constant ($m^3\cdot mol^{-1}\cdot s^{-1}$); C_{i0} is the liquid feed concentration (mol/m^3); and Z is the effective length of the reactor (m).

It should be noted that Eq. 1 was written for a general case. If the reactant a in the liquid is a solute and penetration of the solute through the membrane is negligible, then k_g approaches zero.

The conservation equation at the lumen side can also be formulated as

$$\frac{G}{\Re T}\cdot\frac{dp_i}{dz} = k_{gi}\cdot 2n\pi R_o\cdot(C_i - p_i/H_i) \qquad (i=a,b), \quad (2)$$

with the boundary conditions

$$x = 0, \qquad p_a = 0, \qquad p_b = p_{b0}, \tag{2a}$$

where G is the volumetric flow rate of feed gas (m^3/s); $\Re$ is the gas constant (8.314 J/mol·K); and T is the absolute temperature (K).

Reaction in the Fiber Lumen

$$u\frac{\partial C_i}{\partial z} = D_i\left(\frac{1}{r}\frac{\partial C_i}{\partial r} + \frac{\partial^2 C_i}{\partial r^2}\right) - \upsilon_i k_r C_a C_b$$

or

$$\frac{2Q}{n\pi R^2}\left[1-\left(\frac{r}{R}\right)^2\right]\frac{\partial C_i}{\partial z} = D_i\left(\frac{1}{r}\frac{\partial C_i}{\partial r} + \frac{\partial^2 C_i}{\partial r^2}\right) - \upsilon_i k_r C_a C_b \qquad (i = a,b), \tag{3}$$

where Q is the liquid volumetric flow rate (m^3/s), and D_i is the molecular diffusivity of reactant i in the liquid stream (m^2/s).

The boundary conditions are applied at the center line, at the membrane wall and at the inlet of the membrane reactor

$$r = 0, \qquad \frac{\partial C_i}{\partial r} = 0 \tag{3a}$$

$$r = R, \qquad D_i\frac{\partial C_i}{\partial r} = -k_{gi}(C_i - p_i/H_i) \tag{3b}$$

$$z = 0, \qquad C = C_{i0}. \tag{3c}$$

Again, the boundary condition of Eq. 3b was written for the general case. In case the reactant a in the liquid is a solute, penetration of the solute through the membrane is negligible. Thus, k_g approaches zero.

Together with the mass-balance equation for component i in the shell side, the form of which is the same as Eq. 2 with the exception that R_o is replaced by R, Eq. 3 describes the reactor where the reaction takes place in the fiber lumen.

The overall mass-transfer coefficient, K_{ov}, for reactant a is generally written with the logarithmic-mean concentration difference over the reactor length:

$$J_a = \frac{Q(C_{a0} - C_{ae})}{2n\pi RZ} = K_{oV}\cdot\frac{(C_{a0} - p_a/H) - (C_{ae} - p_a/H)}{\ln\left(\dfrac{C_{a0} - p_a/H}{C_{ae} - p_a/H}\right)}, \tag{4}$$

where J_a is the chemical flux ($mol/m^2 \cdot s$) and C_{ae} is the product concentration given as (Skelland, 1974, p. 154)

$$C_{ae} = \frac{\int_0^R C_a u \cdot 2\pi r\, dr}{\int_0^R u \cdot 2\pi r\, dr} = \frac{4}{R^2}\int_0^R C_a\left[1-(r/R)^2\right] r\, dr \qquad (z = Z). \tag{5}$$

Numerical solution

Model equations representing the reaction in the shell side (Eqs. 1 and 2) or the reaction in the fiber lumen (Eqs. 2 and 3) are the group of highly nonlinear differential equations and can only be solved numerically except for some special cases. By transforming these equations into a group of first-order ordinary differential equations, they can be easily integrated by conventional methods. MATLAB software was used to solve the two sets of equations just cited. The detailed solution method can also be found elsewhere (Tan and Li, 2000).

Solutions for the special cases

In this study, the gas reactant b, which was introduced locally into the liquid phase through the membrane reactor, may be large enough so that its concentration in the liquid is approximately constant throughout the reactor. Therefore, the chemical reaction can be considered as pseudo first-order with respect to the concentration of reactant a, and thus only the mass balance for reactant a needs to be considered. In addition, the amount of the reactant a permeated into the gas phase is considered to be negligible, as the reactant a in liquid is normally a solute. In the case where the reactant a in the liquid is a permeable gaseous reactant, the amount transferred into the gas phase can also be negligible, so long as the gas reactant b introduced into the reactor is considerably higher than the reactant a permeated into the gas phase.

In dimensionless form, the preceding model equations are rewritten as:

Reaction in the Shell Side

$$\frac{dx_a}{d\xi} = \frac{1}{P_e}\frac{d^2x_a}{d\xi^2} - N_m x_a - N_r\left(x_a + \frac{R_c}{1-R_c}\right) \tag{6}$$

with the boundary conditions

$$\xi = 0, \qquad x_a = 1 + \frac{1}{P_e}\frac{dx_a}{d\xi}; \qquad \xi = 1, \qquad \frac{dx_a}{d\xi} = 0. \tag{6a}$$

Reaction in the Fiber Lumen

$$\frac{Gz}{2}(1-\eta^2)\cdot\frac{\partial x_a}{\partial \xi} = \frac{1}{\eta}\frac{\partial x_a}{\partial \eta} + \frac{\partial^2 x_a}{\partial \eta^2} - N_r'\left(x_a + \frac{R_c}{1-R_c}\right), \tag{7}$$

with boundary conditions

$$\eta = 0, \qquad \frac{\partial x_a}{\partial \eta} = 0; \qquad \eta = 1, \qquad \frac{\partial x_a}{\partial \eta} = -N_m' \cdot x_a \tag{7a}$$

$$\xi = 0, \qquad x_a = 1. \tag{7b}$$

The dimensionless variables are defined as

$$\xi = z/Z; \quad \eta = r/R; \quad x_a = \frac{C_a - p_a/H}{C_{a0} - p_a/H}; \quad R_c = \frac{p_a}{HC_{a0}} \tag{8a}$$

$$P_e = \frac{uZ}{D_L}; \quad N_r = \frac{k_r}{u/Z}; \quad N_m = \frac{2k_g/R_o}{u/Z} \cdot \frac{1-\epsilon}{\epsilon} \tag{8b}$$

$$Gz = \frac{4Q}{n\pi D_a Z}; \quad N_r' = \frac{k_r}{D_a/R^2}; \quad N_m' = \frac{k_g R}{D_a}. \tag{8c}$$

The overall mass-transfer coefficient for the reaction in the fiber lumen is generally written in terms of a modified Sherwood number:

$$M_{Sh} = \frac{2K_{ov}R}{D_a} = -\frac{GZ}{4} \ln x_{ae}. \tag{9}$$

Hence, M_{Sh} indicates the performance of the membrane reactor with the reaction in the fiber lumen.

The solution of Eq. 6 (shell-side reaction) can be easily obtained as

$$x_a = \frac{2(1-\beta)(1-\alpha)}{(1-\alpha)^2 - (1+\alpha)^2 \exp(P_e\alpha)} \exp\left(\frac{1+\alpha}{2/P_e}\xi\right) + \frac{2(1-\beta)(1+\alpha)}{(1+\alpha)^2 - (1-\alpha)^2 \exp(-P_e\alpha)} \exp\left(\frac{1-\alpha}{2/P_e}\xi\right) - \beta, \tag{10}$$

where

$$\alpha = \sqrt{1 + \frac{4(N_m + N_r)}{P_e}}; \quad \beta = \frac{N_r}{N_m + N_r} \cdot \frac{R_c}{1-R_c}. \tag{10a}$$

To solve Eq. 7 (reaction in lumen), the technique of separation of variables can be applied and the solution is obtained as

$$x_a(\xi,\eta) = C_0 + \left(C_0 + \frac{R_c}{1-R_c}\right) \sum_{m=1}^{\infty} \frac{N_r'^m}{2^{2m}(m!)^2} \cdot \eta^{2m} + \sum_{j=1}^{\infty} \left[B_j \sum_{m=0}^{\infty} A_{j,2m}\eta^{2m}\right] \cdot \exp\left(-\frac{2\xi}{Gz}\lambda_j^2\right), \tag{11}$$

where C_0, λ_j, A_j, and B_j are obtained from Eqs. A3a, A9, A8, and A10, respectively. A detailed solution of Eq. 11 is given in the Appendix.

Therefore, the product concentration (at $z = Z$) can be calculated for the reaction in the shell side:

$$x_{ae} = \frac{2(1-\beta)(1-\alpha)}{(1-\alpha)^2 - (1+\alpha)^2 \exp(P_e\alpha)} \exp\left(\frac{1+\alpha}{2/P_e}\right) + \frac{2(1-\beta)(1+\alpha)}{(1+\alpha)^2 - (1-\alpha)^2 \exp(-P_e\alpha)} \exp\left(\frac{1-\alpha}{2/P_e}\right) - \beta \tag{12a}$$

and for the reaction in the fiber lumen:

$$x_{ae} = C_0 + 2\left(C_0 + \frac{R_c}{1-R_c}\right) \sum_{m=1}^{\infty} \frac{N_r'^m}{2^{2m}(m!)^2(m+1)(m+2)} + 2\sum_{j=1}^{\infty}\left[B_j \exp\left(-\frac{2\lambda_j^2}{Gz}\right) \sum_{m=0}^{\infty} \frac{A_{j,2m}}{(m+1)(m+2)}\right]. \tag{12b}$$

Obviously, if $R_c = 0$, $N_r' = 0$, and $N_m' \to \infty$, Eq. 12b reduces to the Graetz solution (Skelland, 1974, p. 164). Based on these x_{ae} values, the overall mass-transfer coefficient of the reactor can then be obtained from Eq. 9.

Results and Discussion

We present our analysis on chemical reactions in hollow-fiber membrane modules (reactors) in the following subsections. The fluid flow and the chemical reaction in the shell side of the reactor were studied first, followed by an analysis of the reactor for the chemical reaction in the hollow-fiber lumen. Also, the experimental data in the literature were compared with the modeling values to confirm the validity of the model developed.

Reaction in the shell side

Effect of Axial Dispersion. When the liquid is introduced into the shell side of the reactor, where the reaction also takes place, the axial dispersion becomes an important factor on the reactor performance. Predicted values for this effect are given in Figure 2, where the product concentration, x_{ae}, is plotted against the Peclet numbers. As can be seen, the product concentration decreases as the Peclet number is increased. In addition, the effect of the axial dispersion becomes more pronounced as the value of $N_m + N_r$ is in-

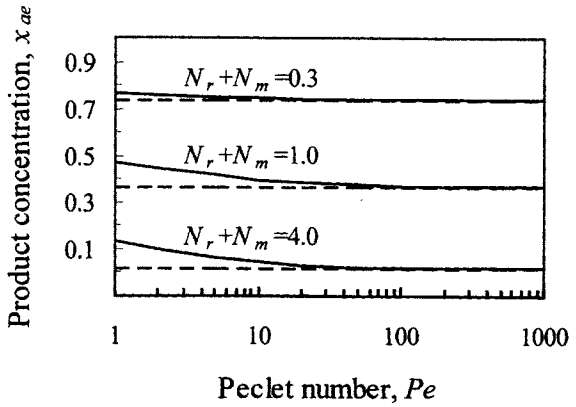

Figure 2. Effect of axial dispersion on the product concentration, x_{ae}, for reaction in shell side of the reactor, $R_c = 0$.

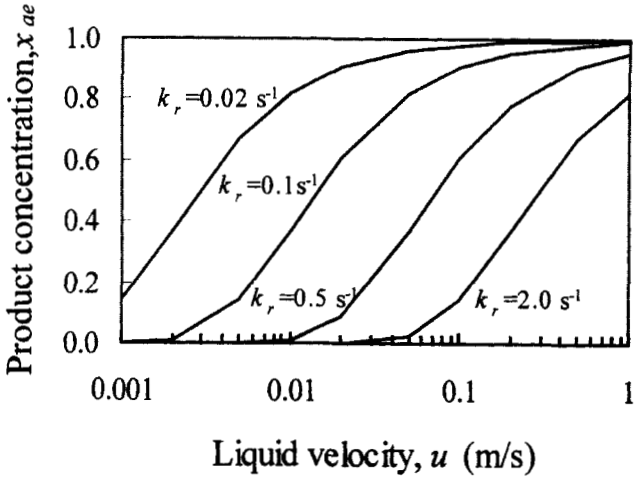

Figure 3. Effect of liquid velocity on the product concentration, x_{ae}, for different reaction constant, $N_c = 0$, $N_m = 0$.

creased. If the axial dispersion is negligible, $Pe \to \infty$, then Eq. 12a reduces to

$$x_{ae} = (1-\beta)\exp[-(N_m + N_r)] - \beta \qquad R_c \neq 0 \quad (13a)$$

$$x_{ae} = \exp[-(N_m + N_r)] \qquad R_c = 0. \quad (13b)$$

The solution of Eq. 13b is also plotted in Figure 2 (dashed line). It can be seen that at a Peclet number greater than 40, the effect of the axial dispersion becomes negligible. Under such a condition, the membrane's coefficient, k_g, or reaction rate constant, k_r, can be evaluated conveniently from Eq. 13. It is interesting to note that the Peclet number, at which the axial dispersion is negligible, is greater than that commonly found in conventional packed-bed reactors (Butts, 1980).

Effect of k_r. The performance of the hollow-fiber reactor with the chemical reaction on the shell side for different k_r values is presented in Figure 3. It can be seen from the figure that for a given value of k_r, the product concentration, x_{ae}, improves as the liquid velocity is decreased. At $k = 2.0$ s^{-1}, the effect of water velocity only becomes noticeable when the water velocity is greater than 0.02 m/s. This is because that at $k = 2.0$ s^{-1} and $u < 0.02$ m/s, the chemical reaction is so fast that all the reactant a (contaminant) is removed due to the chemical reaction. It thus follows that introduction of the chemical reaction will not only improve the purity of the product stream, but also increase the capacity of the reactor for contaminant removal.

Reaction in the fiber lumen

Concentration Profile. For the chemical reaction, which takes place in the fiber lumen, the effect of the reaction on the concentration profiles of the reactant a in the hollow-fiber lumen can be realized. Figures 4a and 4b show typical three-dimensional concentration profiles of x_a for two different reaction moduli, $N_r' = 1$ and $N_r' = 5$, respectively. Because the reaction modulus N_r' equals 1 (slow reaction), the concentration, x_a, decreases from the center line to the membrane wall

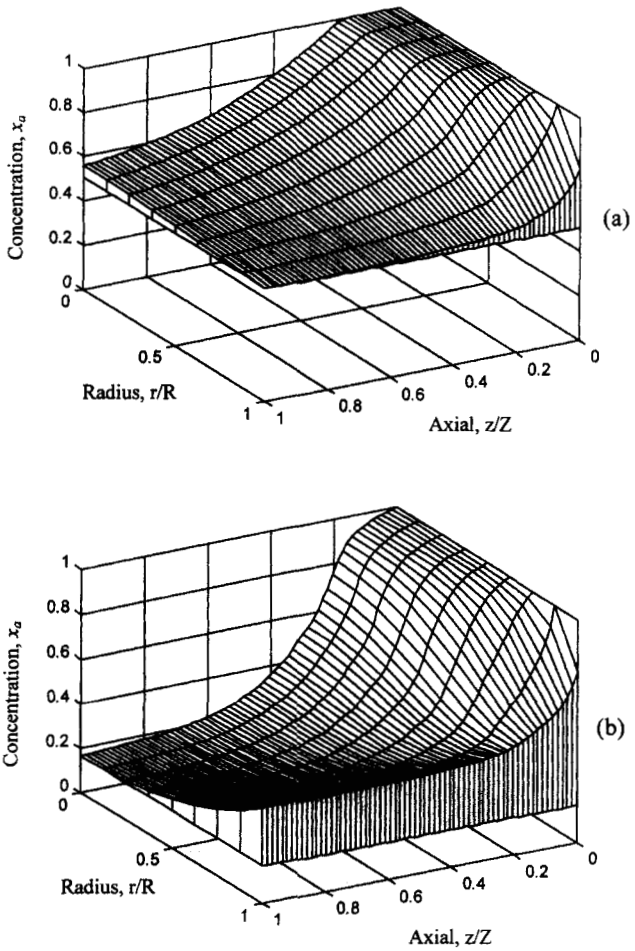

Figure 4. Concentration profiles for different reaction modulus, $Gz = 5$, $R_c = 0.5$: (a) $N_r' = 1$; (b) $N_r' = 5$.

along the whole fiber length. This suggests that the disappearance of the reactant a is not only due to the chemical reaction, but also to the mass transfer (gas permeation) that always takes place from the fiber lumen to the shell side of the reactor. As the value of N_r' increases to 5 (fast reaction), the concentration, x_a, also decreases from the center line to the membrane wall at $z/Z < 0.7$. However, at $z/Z > 0.7$ the reverse becomes true. This phenomenon can be attributed to the fast reaction in the fiber lumen. Because of the fast chemical reaction, the concentration of the reactant a in the fiber lumen reduces dramatically along the fiber length. At $z/Z > 0.7$, the concentration of the reactant a in the shell side, p_a, resulting from the gas permeation becomes greater than that in the hollow-fiber lumen, HC_a. Under such conditions the reversed mass transfer (gas permeation) takes place, resulting in the reverse concentration profile toward the outlet of the reactor.

When the contaminant (reactant a) in water is a gaseous reactant, the reversed mass transfer inevitably takes place at high N_r' values. Such a reversed mass transfer reduces the reactor performance and should always be prevented. To avoid this, one can reduce the value of the concentration modulus, R_c, defined as the concentration ratio between the

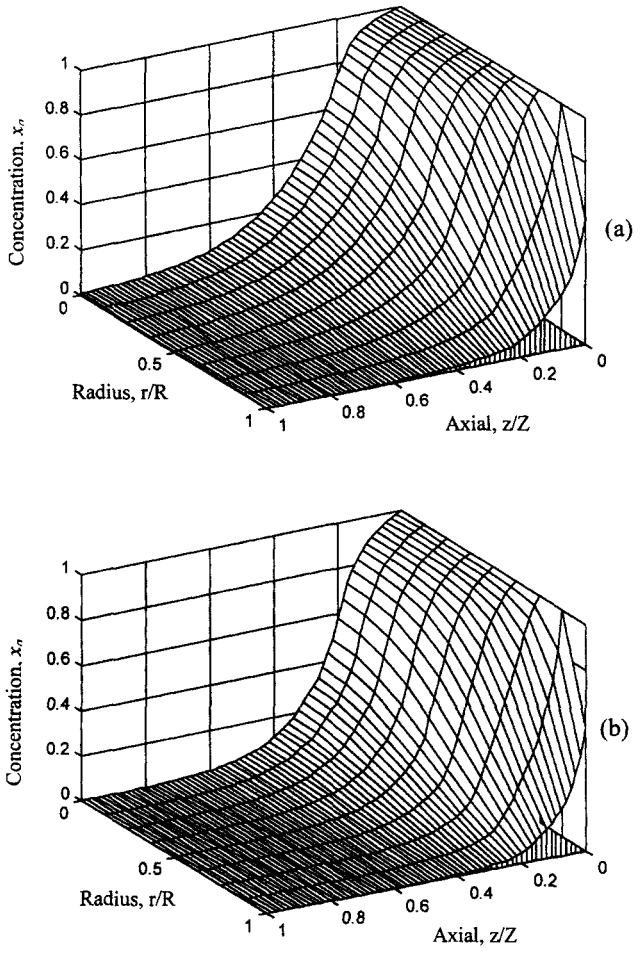

Figure 5. Concentration profiles for different reaction modulus, $Gz = 5$, $R_c = 0$: (a) $Nr = 5$: (b) $Nr = 10$.

gas phase and the inlet liquid phase, $R_c = p_a/HC_{a0}$, which directly reflects the level of the p_a in the shell side. As shown in Figure 5, when the R_c value approaches zero, no reversed mass transfer could take place, even when the value of the reaction modulus, N_r', is increased to 10 (Figure 5b).

Reactor Performance. Since the chemical reaction occurs in the fiber lumen, the modified Sherwood number, M_{Sh}, defined in Eq. 9, can be used to evaluate the reactor performance. Figure 6 plots the modified Sherwood number vs. the Graetz number for the different reaction-rate constant, k_r, shown as the reaction modulus, N_r'. As can be expected, the modified Sherwood number increases with the Graetz number due to the increase of the liquid flow rate in the fiber lumen. It can also be seen that the modified Sherwood number increases as the reaction-rate constant is increased, indicating that the reactor performance is improved due to the chemical reaction.

Also in Figure 6, the Leveque solution (solid line) and Graetz solution (dotted line) are plotted. At low Graetz number, the Leveque solution predicts a lower modified Sherwood number due to its limiting assumptions used in the model derivation. In addition, a very small difference was observed between the present solution at $N_r' = 0$ and the Graetz

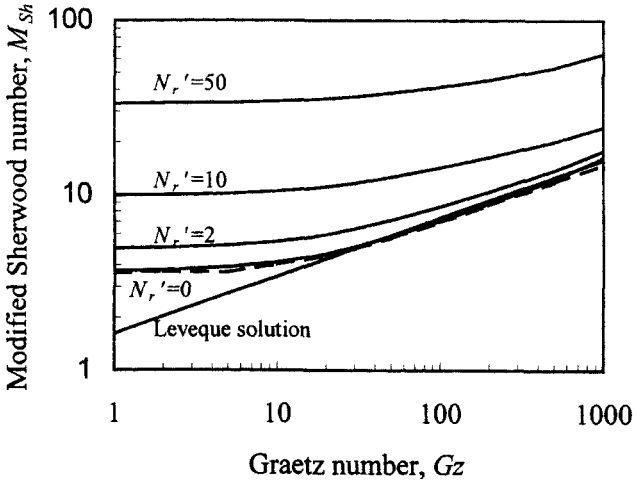

Figure 6. Modified Sherwood number vs. Graetz number for different reaction modulus, $R_c = 0$, $N_m' = 840$.

solution. This is because the Graetz solution is based on the assumption of infinite mass-transfer modulus, that is, $N_m' \to \infty$, while the present solution was calculated at $N_m' = 840$. This suggests that, at $N_m' = 840$, the membrane resistance is negligible.

Comparison with experimental data

Experimental data obtained by Shanbhag et al. (1995) and Sinha (2000) have been employed for comparison with the theoretical models developed in this study.

Shanbhag et al. (1995) conducted an ozonation experiment on wastewater treatment using a hollow-fiber membrane module where the aqueous feed containing nitrobenzene was passed through the shell side of the module, while ozone-containing oxygen was introduced into the fiber lumen. The hollow-fiber membrane acted as an ozone distributor. Therefore, the chemical reaction between ozone and nitrobenzene takes place at the shell side. During the calculation, the membrane transfer coefficient for the liquid contaminant is considered to be zero, as the permeability of the contaminant is small and negligible for the silicone membrane employed. Also, the elementary reaction with the reaction-rate constant given by Shanbhag et al. (1995) was directly employed for calculation. In addition, the axial dispersion coefficient is estimated using the following equation (Zee et al., 1995):

$$D_L = (1.2 \times 10^{-4}\text{m})u(1-\epsilon)^{-1/3}. \qquad (14)$$

The experimental data and theoretical results are shown in Figure 7. It can be seen that they are in excellent agreement. Due to the efficient distribution of the ozone, the concentration of the ozone in liquid can be considered to be constant throughout the hollow-fiber module. As can be seen in the figure, the simulation results under assumption of a pseudo-first-order reaction (solid line), that is, constant ozone concentration in liquid, provides an almost identical solution compared to the results calculated from the second-order reaction (dashed line).

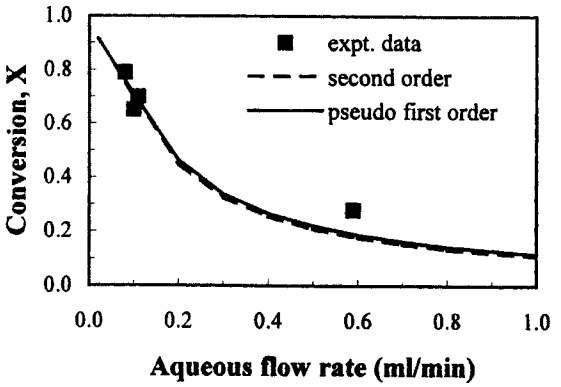

Figure 7. Theoretical results vs. experimental data: removal of hazardous organic compounds in water by nonporous silica hollow-fiber membrane modules.

Sihna (2000) studied a UV membrane reactor for dissolved oxygen (DO) removal from water. The water containing DO was fed into the fiber lumen while purified hydrogen was introduced into the shell side. Therefore, the DO diffused through the hollow-fiber membranes into the gas stream and was purged by the hydrogen stream flowing in the shell side. Simultaneously, the hydrogen gas also diffuses through the hollow-fiber membrane and dissolves into the water. Under the catalysis of the UV light, the dissolved hydrogen reacts with the remaining dissolved oxygen to form water. Obviously, the reaction between the dissolved oxygen and hydrogen takes place in the hollow-fiber lumen. When the hydrogen is present in excess of the stoichiometric requirement in water, the pseudo-first-order reaction with respect to the dissolved oxygen concentration would be expected to prevail (Suppiah et al., 1988).

The experimental data and theoretical results are shown in Figure 8. In Figure 8a $p_{H_2} = 0$ indicates that pure nitrogen instead of hydrogen is fed as a purge gas, and thus no reaction would take place in the lumen side. The reaction constants estimated using the model developed are about 0.0913 s^{-1} and 0.1505 s^{-1} when the hydrogen pressure at the shell side are operated at 1 atm and 3 atm, respectively. Such a difference is obviously the result of the increased dissolved hydrogen concentration in water resulting from the elevation of the hydrogen gas pressure at the shell side.

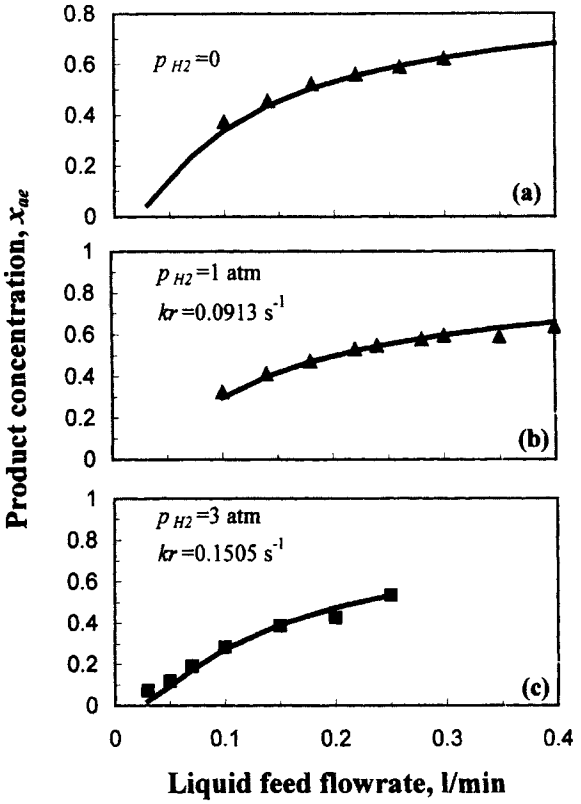

Figure 8. Theorectical results vs. experimental data: DO removal from water by UV membrane reactor.

Conclusions

The mathematical model has been developed to describe hollow-fiber membrane reactors where the membrane functions as a reactant distributor. The analytical solutions to the model equations for the chemical reaction taking place either in the hollow-fiber lumen or in the shell side were obtained on condition that the reaction is first order or pseudo first order, which is usually true for the water-treatment processes. For the reaction in the shell side, axial dispersion must be taken into consideration, but can be neglected when $Pe > 40$. When the contaminant (reactant *a*) in water is a gaseous reactant, the mass-transfer direction may be reversed due to the fast chemical reaction. Based on the solution method developed, the reaction kinetic parameters can be obtained conveniently from the hollow-fiber reactors once the reaction mechanism is known. Experimental results in the literature obtained from different reactors (modules) with different dimensions for the removal of dissolved oxygen or hazardous organic compounds from water are in satisfactory agreement with the theoretical solution.

Notation

A = cross-sectional area of the reactor, m^2
C_a = liquid-phase concentration, mol/m^3
C_{a0} = liquid-feed concentration, mol/m^3
C_{ae} = product concentration, mol/m^3
D_L = axial-dispersion coefficient, m^2/s
D_a = diffusivity in liquid stream, m^2/s
d_o = outer diameter of the hollow fiber, m
G = volumetric flow rate of feed gas, m^3/s
Gz = Graetz number, $Gz = 4Q/n\pi D_a Z$
H = Henry constant, $atm \cdot m^3/mol$
J_A = chemical flux, $mol/m^2 \cdot s$
k_g = mass-transfer coefficient, m/s
k_r = reaction-rate constant, s^{-1}
K_{oV} = overall mass-transfer coefficient, m/s
N = number of hollow fibers
N_m = mass-transfer modulus defined by Eq. 8b
N'_m = modified mass-transfer modulus, $N'_m = k_g R/D_a$
N_r = chemical-reaction modulus, $N_r = k_r Z/u$
N'_r = modified reaction modulus, $N'_r = k_r R^2/D_a$
p_a = partial pressure in gas phase, atm
Pe = Peclet number, $Pe = uZ/D_L$
Q = volumetric flow rate of liquid feed, m^3/s
R_o = outer radius of the hollow fiber, m

R = inner radius of the hollow fiber, m
R = radius variable, m
R_c = dimensionless gas phase concentration, $R_c = p_a/HC_{a0}$
M_{Sh} = modified Sherwood number, $M_{Sh} = 2K_{oV}R/D_a$
U = liquid superficial velocity, m/s
v_i = chemical reaction stoichiometric number
X = conversion of nitrobenzene
x_a = dimensionless liquid concentration
x_{ae} = dimensionless outlet concentration
Z = active length of the module, m
Z = axial-length variable, m

Greek letters

α, β = constants defined by Eq. 10a
η = dimensionless radius
ϵ = void fraction of the module
ξ = dimensionless axial length

Literature Cited

Butts, T. J., *Reaction Kinetics and Reactor Design*, Prentice Hall, Englewood Cliffs, NJ (1980).
Chang, H. N., and S. Furusaki, "Membrane Bioreactors: Present and Prospects," *Adv. Biochem. Eng. Biotechnol.*, **44**, 27 (1991).
Cheng, S., and X. Shuai, "Simulation of a Catalytic Membrane Reactor for Oxidative Coupling of Methane," *AIChE J.*, **41**, 1598 (1995).
Coronas, J., M. Menendez, and J. Santamaria, "Methane Oxidative Coupling Using Porous Ceramic Membrane Reactors—II Reaction Studies," *Chem. Eng. Sci.*, **49**, 2015 (1994a).
Coronas, J., M. Menendez, and J. Santamaria, "Development of Ceramic Membrane Reactors with a Non-Uniform Permeation Pattern, Application to Methane Oxidative Coupling," *Chem. Eng. Sci.*, **49**, 4749 (1994b).
Coronas, J., A. Gonzalo, D. Lafarga, and M. Menendez, "Effect of the Membrane Activity on the Performance of a Catalytic Membrane Reactor," *AIChE J.*, **43**, 3095 (1997).
Eng, D., and M. Stoukides, "Catalytic and Electrocatalytic Methane Oxidation with Solid Oxide Membranes," *Catal. Rev. Sci. Eng.*, **33**, 375 (1991).
Hsieh, H. P., "Inorganic Membrane Reactors," *Catal. Rev.-Sci. Eng.*, **33**, 1 (1991).
Li, K., I. Chua, W. J. Ng, and W. K. Teo, "Removal of Dissolved Oxygen in Ultrapure Water Production Using a Membrane Reactor," *Chem. Eng. Sci.*, **50**, 3547 (1995).
Michaels, A. S., "New Separation Technique for the CPI," *Chem. Eng. Prog.*, **64**, 31 (1968).
Mohan, K., and R. Govind, "Analysis of Equilibrium Shift in Isothermal Reactors With a Permselective Wall," *AIChE J.*, **34**, 1493 (1988).
Pfefferle, W. C., "Process for Dehydrogenation," U.S. Patent No. 3,290,406 (1966).
Reyes, S. C., E. Iglesia, and C. P. Kelkar, "Kinetic-Transport Models of Bimodal Reaction Sequences: I. Homogeneous and Heterogeneous Pathways in Oxidative Coupling of Methane," *Chem. Eng. Sci.*, **48**, 2643 (1993a).
Reyes, S. C., C. P. Kelkar, and E. Iglesia, "Kinetic-Transport Models and the Design of Catalyst and Reactors for the Oxidative Coupling of Methane," *Catal. Lett.*, **19**, 167 (1993b).
Shanbhag, P. V., A. K. Guha, and K. K. Sirkar, "Single-Phase Membrane Ozonation of Hazardous Organic Compounds in Aqueous Stream," *J. Hazardous Mat.*, **41**, 95 (1995).
Shanbhag, P. V., A. K. Guha, and K. K. Sirkar, "Membrane-Based Ozonation of Organic Compounds," *Ind. Eng. Chem. Res.*, **37**, 4388 (1998).
Shu, J., B. P. A. Grandjean, A. Van Neste, and S. Kallaguine, "Catalytic Palladium-Based Membrane Reactors: A Review," *Can. J. Chem. Eng.*, **69**, 1036 (1991).
Sinha, V., "Novel Membrane Reactor for Dissolved Oxygen Removal in Ultrapure Water Production," MEng Thesis, National Univ. of Singapore, Singapore (2000).
Skelland, A. H. P., *Diffusional Mass Transfer*, Wiley, New York (1974).
Suppiah, S., K. J. Kutchcoskie, P. V. Balakrishnan, and K. T. Chuang, "Dissolved Oxygen Removal by Combination with Hydrogen Using Wetproofed Catalysts," *Can. J. Chem. Eng.*, **66**, 849 (1988).
Tan, X., and K. Li, "Investigation of Novel Membrane Reactors for Removal of Dissolved Oxygen from Water," *Chem. Eng. Sci.*, **55**, 1213 (2000).
Tsai, C.-Y., Y. H. Ma, W. R. Moser, and A. G. Dixon, "Modeling and Simulation of a Nonisothermal Catalytic Membrane Reactor," *Chem. Eng. Commun.*, **134**, 107 (1995).
Van Zee, G., R. Veenstra, and J. de Graauw, "Axial Dispersion in Packed Fiber Beds," *Chem. Eng. J.*, **58**, 245 (1995).
Wood, B. J., "Dehydrogenation of Cyclohexane on a Hydrogen-Porous Membrane," *J. Catal.*, **11**, 30 (1968).

Appendix

The solution to the model equation (Eq. 7) can be written as

$$x_a(\xi,\eta) = \psi(\xi,\eta) + \omega(\eta), \tag{A1}$$

in which the function $\omega(\eta)$ satisfies the following equation:

$$\frac{1}{\eta}\frac{d\omega}{d\eta} + \frac{d^2\omega}{d\eta^2} - N_r'\omega + \frac{N_r'}{R_c - 1} = 0, \tag{A2}$$

with boundary conditions:

$$\eta = 0, \quad \frac{d\omega}{d\eta} = 0; \qquad \eta = 1, \quad \frac{d\omega}{d\eta} = -N_m'\cdot\omega. \tag{A2a}$$

The model has a solution of infinite series form:

$$\omega(\eta) = C_0 + \left(C_0 + \frac{R_c}{1-R_c}\right)\sum_{m=1}^{\infty}\frac{N_r'^m}{2^{2m}(m!)^2}\cdot\eta^{2m}, \tag{A3}$$

where C_0 is derived from the boundary condition (Eq. 5a) as follows:

$$C_0 = \frac{R_c}{R_c - 1}\cdot\frac{\sum_{m=1}^{\infty}\left(1+\frac{2m}{N_m'}\right)\frac{N_r'^m}{2^{2m}(m!)^2}}{1+\sum_{m=1}^{\infty}\left(1+\frac{2m}{N_m'}\right)\frac{N_r'^m}{2^{2m}(m!)^2}}. \tag{A3a}$$

Inserting Eq. A1 into Eq. 5 gives a partial differential equation in the function ψ,

$$\frac{Gz}{2}(1-\eta^2)\cdot\frac{\partial\psi}{\partial\xi} = \frac{1}{\eta}\frac{\partial\psi}{\partial\eta} + \frac{\partial^2\psi}{\partial\eta^2} - N_r'\psi, \tag{A4}$$

with boundary and initial conditions:

$$\eta = 0, \quad \frac{\partial\psi}{\partial\eta} = 0; \qquad \eta = 1, \quad \frac{\partial\psi}{\partial\eta} = -N_m'\cdot\psi \tag{A4a}$$

$$\xi = 0, \quad \psi = 1 - \omega(\eta). \tag{A4b}$$

The separation-of-variables technique is applied to Eq. A4,

and its solution should be of the following form:

$$\psi(\xi,\eta) = \theta(\eta)\cdot\phi(\xi)$$

or

$$\psi(\xi,\eta) = \sum_{j=1}^{\infty} B_j\theta_j(\eta)\cdot\exp\left(-\frac{2\xi}{GZ}\lambda_j^2\right), \qquad \text{(A5)}$$

where $\lambda_1, \lambda_2, \ldots, \lambda_j, \ldots$ are the eigenvalues of the following boundary-value problem of the Sturm-Liouville type for θ in increasing order, and $\theta_j(\eta)$ denotes the eigenfunction corresponding to λ_j, namely,

$$\frac{1}{\eta}\frac{d}{d\eta}\left(\eta\frac{d\theta(\eta)}{d\eta}\right) + \left[(1-\eta^2)\lambda^2 - N_r'\right]\theta(\eta) = 0, \qquad \text{(A6)}$$

with boundary conditions:

$$\eta = 0, \quad \frac{d\theta}{\partial\eta} = 0; \qquad \eta = 1, \quad \frac{d\theta}{d\eta} + N_m'\cdot\theta = 0. \qquad \text{(A6a)}$$

The coefficients B_j in the expansion are given by the following expression, which requires the series in Eq. A5 to satisfy the initial-condition equation (Eq. A4b), $\sum_{j=1}^{\infty} B_j\theta_j(\eta) = 1 - \omega(\eta)$:

$$B_j = \frac{\int_0^1[1-\omega(\eta)]\theta_j(1-\eta^2)\eta\,d\eta}{\int_0^1\theta_j^2(1-\eta^2)\eta\,d\eta}. \qquad \text{(A7)}$$

On the other hand, the solution to Eq. A6 can also be written by an infinite series:

$$\theta(\eta) = \sum_{m=0}^{\infty} A_{2m}\eta^{2m}, \qquad \text{(A8)}$$

in which the coefficients A_{2m} are obtained by substituting Eq. A8 into Eq. A6:

$$A_0 = 1; \quad A_2 = -\frac{1}{2^2}(\lambda^2 - N_r') \qquad \text{(A8a)}$$

$$A_{2m} = -\frac{1}{(2m)^2}\left[(\lambda^2 - N_r')A_{2m-2} - \lambda^2 A_{2m-4}\right], \quad m = 2, 3, 4, \ldots . \qquad \text{(A8b)}$$

Since the series (Eq. A8) should satisfy the boundary condition (Eq. A6a), then it gives

$$f(\lambda^2) = 1 + \sum_{m=1}^{\infty} A_{2m}\left(1 + \frac{2m}{N_m'}\right) = 0. \qquad \text{(A9)}$$

Thus, the eigenvalues can be calculated by solving Eq. A9 using a trial-and-error procedure.

Meanwhile, substituting Eqs. A3 and A8 into Eq. A7 and rearranging gives

$$B_j = \frac{\left(1+\frac{R_c}{1-R_c}\right)\sum_{m=0}^{\infty}\frac{A_{j,2m}}{(m+1)(m+2)} - \left(C_o + \frac{R_c}{1-R_c}\right)\sum_{m=0}^{\infty}\left[A_{j,2m}\sum_{k=1}^{\infty}\frac{N_r'^k}{2^{2k}(k!)^2(m+k+1)(m+k+2)}\right]}{\sum_{m=0}^{\infty}\frac{\sum_{k=0}^{m}A_{j,2k}A_{j,2(m-k)}}{(m+1)(m+2)}}. \qquad \text{(A10)}$$

Combining Eqs. A3, A5, and A8 gives the final solution to the model Eq. 6 as

$$x_a(\xi,\eta) = C_0 + \left(C_0 + \frac{R_c}{1-R_c}\right)\sum_{m=1}^{\infty}\frac{N_r'^m}{2^{2m}(m!)^2}\cdot\eta^{2m} + \sum_{j=1}^{\infty}\left[B_j\sum_{m=0}^{\infty}A_{j,2m}\eta^{2m}\right]\cdot\exp\left(-\frac{2\xi}{Gz}\lambda_j^2\right). \qquad \text{(A11)}$$

Manuscript received April 18, 2000, and revision received July 5, 2000.